Supplemental Methods

Cell culture

Human cell lines were purchased from the German Collection of Microorganisms and Cell Cultures (DSMZ) and maintained according to the supplier's instructions. Adult CD34+ HSPCs were obtained from mobilized peripheral blood from anonymous healthy donors and enriched using anti-CD34 immunomagnetic microbeads. Media promoting the megakaryocytic differentiation of HSPCs has been previously described[1]. Media promoting the erythroid differentiation of HSPCs consisted of Stemspan SFEM II supplemented with 1% penicillin/streptomycin, 1% L-glutamine, 2µM dexamethasone, 1µM β-estradiol (Sigma Aldrich), 1U/ml EPO, 5ng/mL IL-3 and 12ng/mL SCF. Human PDXs were cultured in Stemspan SFEM II supplemented with 1% penicillin/streptomycin, 100ng/ml SCF, 100ng/ml FLT3-L, 20ng/ml IL-6, 50ng/ml TPO, 0.75µM StemRegenin1 and 35nM UM171. All cytokines were purchased from Peprotech. All cells were maintained at 37°C. Cells were transduced with concentrated viral particles in the presence of 2-5µg/ml polybrene. Primary human and murine HSPCs were transduced in Retronectin-coated plates according to manufacturer's instructions (Takara Bio). Murine *Gata1s*-FLCs were prepared and cultured as previously described[2] and maintained for at least 21 days. Day 0 was defined as 96 hours post transduction or upon doxycycline addition (500ng/mL). Colony forming unit (CFU) assays were performed as described previously[3,4], either in complete (HSC003 and HSC007, R&D Systems) or low (HSC006, R&D Systems; supplemented with 20ng mL Thpo) cytokine conditions.

Micrographs

Micrographs were obtained with a Keyence BZ-9000 Microscope using the BZ-II viewer, and images were processed with the BZ-II Analyzer software. Micrographs of sternum, spleen and liver samples from leukemic mice were obtained with an Axioplan microscope (Carl Zeiss) and processed with the Zen Lite 2012 software following hematoxylin&eosin staining.

Lentiviral production

Lentiviral particles were generated by co-transfecting HEK293T cells with the corresponding expression constructs, pMD2.G and psPAX2 (Addgene #12259 and #12260), via the polyethyleneimine transfection method as previously described[3]. shRNAs were designed using the miR-N tool[5] applying the SENSOR design rules[6] and cloned into a SIN40C.SFFV.dTomato.miR30n backbone[7]. DNA sequences corresponding to the different miRNAs[3] were cloned into SIN40C.SFFV.miR30n backbones containing different fluorescent proteins (dTomato, GFP and mTagBFP2, respectively). A non-silencing shRNA against Renilla luciferase in the miR-30n backbone was used as a control (sh-ctrl)[7]. Codon-optimized

cDNAs were similarly cloned into the same SIN40C.SFFV backbone encoding GFP or dTomato as a fluorescent reporter. For inducible expression, a doxycycline-inducible SIN40C.TRE vector was used. All plasmids generated in this study have been deposited at Addgene and are listed in **Supplemental Table 1**.

shRNA positive selection screening

2 million Gata1s-FLCs were transduced with the miR-125b-mimicking shRNA library (MOI=0.3) to achieve sufficient representation (<500-fold of X shRNAs). Samples were harvested after 4 and 30 days in culture, and gDNA was extracted using the QIAamp DNA Blood Mini Kit (Qiagen). The shRNA amplicon was PCR-amplified using primers containing the p5 and p7 adaptor sequences, gel-purified and sequenced (single-end) on an Illumina HiSeq 2500. We used model-based analysis of genome-wide CRISPR/Cas9 knockout (MAGeCK)[8] to identify hits from the shRNA screen. Custom R scripts were used for demultiplexing double barcoded reads; guides with fewer than 20 reads in ≥75% of all samples were excluded. Raw read counts were passed to the mageck test command using default parameters. Day 30 samples were compared to day 4 (n=12) to determine enrichment. Genes with a p-value <0.05 as determined by MAGeCK were deemed significant.

Proteomic analysis

Total cell lysis and Western blotting were performed as previously described [4]. Blots were developed using Amersham™ ECL Prime Western Blotting Detection Reagent (Thermo Fisher Scientific). CoIP of endogenous ARID3A was performed on CMK cells using Anti-ARID3A antibodies coupled to Novex™ DYNAL™ Dynabeads™ Protein G (Thermo Fisher Scientific). After cell lysis and affinity pulldown, proteins were eluted and subjected to proteolysis with trypsin (Promega) according to the filter-aided sample preparation (FASP) protocol[9]. Samples were analyzed by LC/MS/MS using a U3000 nano-HPLC system coupled to a Q-Exactive Plus mass spectrometer (Thermo Fisher Scientific). Raw data were processed using Proteome Discoverer 2.4 (Thermo Fisher Scientific). MS/MS data were searched against the Uniprot database (version Nov. 2019, tax. *Homo sapiens*, 73801 entries)[10] using Sequest-HT[11]. Label-free quantification of proteins was based on extracted peak areas of corresponding peptide precursor ions.

3'UTR binding assay

To evaluate binding of miR-125b to the 3'UTR of the *ARID3A/Arid3a* mRNA, we cloned the 3'UTRs containing the miR-125b binding sites into a SIN40C.EFS.eGFP.pre lentiviral backbone downstream of the eGFP cassette. A 3'UTR with 3 exchanged nucleotides in the predicted miR-125b binding sites was used as mutated control. After lentiviral transduction, HEL cells were FACS-sorted and transduced with miR-125b or a miR-control. Knockdown efficiency was defined as previously described[12].

Flow cytometry and sorting

Flow cytometry was performed on a CytoFLEX flow cytometer (Beckman Coulter) and the data were analyzed in Kaluza 1.5 (Beckman Coulter). Antibodies are listed in **Supplemental Table 1**. Cell sorting was performed on a BD FACSAria™ II Flow Cytometer (BD Biosciences). Apoptosis was measured using the Annexin V Apoptosis Detection Kit II with APC-Annexin V (BD Biosciences) or PE-Cy7-Annexin V kit (Thermo Fisher Scientific). Cell cycle analysis was performed using the BrdU Flow Kit (BD Biosciences) and Alexa Fluor 647 Anti-BrdU (BD Biosciences) or PE-Cy7 anti-BrdU (Biolegend). Both assays were performed according to manufacturers' instructions.

Gene expression profiling

sgLuc- transduced FLCs were FACS-sorted three days after transduction; transduced CMK or *Gata1s*-FLCs were FACS-sorted 2, 10 and 13 days after doxycycline induction (0.5µg/mL). RNA was prepared using the Quick-RNA™ Miniprep Kit (Zymo Research). RNA-Sequencing was performed by Novogene Company, Ltd. A minimum amount of 150ng RNA was used as input material for the RNA sample preparations. Sequencing libraries were generated using NEBNext® UltraTM RNA Library Prep Kit for Illumina® (New England Biolabs) and sequenced on an Illumina NovaSeq using a paired-end 150bp system. Raw FASTQ data (raw reads) were first pre-processed using fastp[13] and then further processed as previously described[14]. Differential expression analysis was performed using the DESeq2 package in R[15]. The resulting P values were adjusted using the Benjamini and Hochberg's approach for controlling the False Discovery Rate (FDR)[16]. Genes with an adjusted P value <0.05 were considered differentially expressed. Functional enrichments were calculated via gene set enrichment analysis (GSEA; v4.0)[17] using previously described gene sets and curated ML-DS signatures[7]. Human gene symbols were mapped to murine gene symbols using orthologue annotations provided by Ensembl[18], considering only one-to-one orthologue relationships.

To quantify miR-125b expression levels, *Gata1s*-FLCs were FACS-sorted 72 hours after transduction or 48h post doxycycline induction. RNA was prepared using the Quick-RNA™ Miniprep Kit (Zymo Research), and TaqMan Advanced miRNA Assays were performed using the TaqMan™ MicroRNA Reverse Transcription Kit and TaqMan™ Universal PCR-Mastermix (Thermo Fisher Scientific) with primers specific for miR-125b (Assay ID #000449) and U6 (Assay ID #000435).

Chromatin profiling

miR-125b-*Gata1s*-FLCs expressing doxycycline-inducible A*rid3a-FLAG* or *LUC* cDNA were FACS-purified after 48 hours of doxycycline induction. CUT&RUN was performed as previously described[19,20]. 200,000 cells were sorted and incubated with the following antibodies: rabbit anti-DRIL-1 (Abcam), rabbit anti-GATA1 (Abcam), rabbit anti-SMAD2 and anti-SMAD3 (Cell Signalling) and rabbit anti-IgG (Diagenode).

The pAG/MNase nuclease (Addgene #123461) was produced and purified as previously described[19] after removal of the HA tag. Illumina libraries were constructed from cleaved DNA (CUT&RUN) and sequenced by Novogene Company, Ltd. on an Illumina NovaSeq 6000 (150 bp paired-end reads). For processing the raw data, we used Trimmomatic (v0.39)[21] to remove adapter sequences, followed by Kseq[22] to trim reads containing ≤6 bp of adapter sequence, which are not effectively handled by Trimmomatic. Trimmed reads were aligned to mm10 using bowtie 2 (v2.3.5.1.)[23]. The resulting SAM files were converted into BAM format and sorted and indexed using Samtools (v1.3.1.)[24]. Normalized bigwig tracks (reads per kilobase per million reads [RPKM]) were generated using bamCoverage from deepTools (v3.5.1.)[25]. The processed data were viewed in the Integrated Genomics Viewer (IGV)[26]. SEACR (v1.1)[27] was used to call significantly enriched peaks. HOMER (v4.11.1.)[28] was used to identify overlapping peaks; binding sites were defined as the peak summit ± 500 bp[29]. Heatmaps were generated using deeptools (v3.5.1.)[25].

ATAC-Seq

We performed assay for transposase accessible chromatin sequencing (ATAC-seq) as previously described[30,31]. 50,000 miR-125b-*Gata1s*-FLCs expressing doxycycline-inducible *Arid3a-FLAG* or *LUC* cDNA were FACS-purified after 48 hours of doxycycline induction and processed using the Illumina Tagment DNA Enzyme and Buffer Kit (Illumina). The resulting libraries were sequenced by Novogene Company, Ltd. on an Illumina NovaSeq 6000 (150 bp paired end reads). The data processing was also performed by Novogene: in brief, raw reads were trimmed and filtered using Skewer[32] and clean reads were aligned to mm10 with BWA[33]. Mitochondrial reads were removed prior to subsequent analysis. Normalized pileups were generated using deepTools[25] and viewed in the Integrated Genomics Viewer (IGV)[26].

Patient survival analysis

Event-free survival (EFS) was defined as time from diagnosis to the first event or last follow-up. Events were death from any cause, failure to achieve remission, relapse, and secondary malignancy. Failure to achieve remission was considered as an event on day 0. Overall survival was defined as the time between diagnosis and death from any cause or last follow-up. The Kaplan-Meier method was used to estimate survival rates[34]. Differences were compared using the 2-sided log-rank test[35], and standard errors were obtained using the Greenwood formula. The DESeq2 package was used to normalize and variance-stabilize RNA-sequencing read count data[15]. The pediatric AML data set further required batch correction, for which we used the sva package[36]. Normalized (and batch-corrected) expression of *ARID3A* was taken as a continuous variable in the survival model. For patient stratification, the optimal cutoff point was determined using maximally selected log-rank statistics as implemented in

the maxstat R package (http://cran.r-project.org/web/packages/maxstat/index.html). The calculated cutoff for EFS was used for both overall survival and EFS analyses. We relied on R Version 3.6.1 (http://www.r-project.org/) for all of the above computations. Multivariate analysis was performed using the Cox proportional hazards model[37] and SAS 9.4 was used to compute hazard ratios and 95% CIs of the relative risk for the respective prognostic factors (*ARID3A* expression, dataset, cytogenetic risk group, gender, age, white blood cell count [WBC]).

Supplemental Tables

Supplemental Table 1: List of reagents and resources

Supplemental Table 2: Patient sample characteristics

Supplemental Table 3: Targets and sequences of the miR-125b-mimic shRNA library

Supplemental Table 4: Enrichment scores from the shRNA-based positive selection screen

Supplemental Table 5: GSEA results of global gene expression profiling after overexpression of miR-125b in *Gata1s*-FLCs

Supplemental Table 6: List of shRNA targeting *ARID3A*/*Arid3a*

Supplemental Table 7: GSEA results of global gene expression profiling after modulation of *Arid3a* in *Gata1s*-FLCs

Supplemental Table 8: Pairwise analysis of LC-MS/MS

Supplemental Table 9: GSEA results of global gene expression profiling after overexpression of *ARID3A* in CMK

Supplemental Table 10: Multivariate cox regression analysis

Supplemental Table 2: Patient sample characteristics

	gender	age at diagnosis (years)	WBC (x109/L)	hemoglobin (g/dl)	BM blasts (%)	CNS	SCT	molecular genetics	Cytogenetics (karyotype)	response	relapse
ML-DS PDX#1	m	2 1/6	32500	7.9	70.5	no	yes	GATA1 mutation	47,XY,t(3;13)(q?26;q?13~14) del(13)(q?14q22),+21c[cp14]/ 47,sl,del?(15)(q?)[cp2]/46,XY[1]	NR, CCR:after SCT	no
ML-DS PDX#2	m	1 1/3	4800	12	10.5	no	no	GATA1 mutation	k.A.	CCR	no
ML-DS PDX#3	f	1 1/12	168000	7.1	16	no	no	NRAS mutation	k.A.	CCR	no
AMKL PDX#1	m	1	40000	9.9	64	no	yes	KMT2A mutation	46,XY[15].nuc ish 3q26(EVI1x2)[100/100], 8q22(RUNX1T1x2),21q22(RUNX1x2)[98/100], 11 q23(MLLx2)[99/100], 16q22(CBFBx2)[100/100] 17q21.1(RARAx2)[100/100]	CCR	yes
AMKL PDX#2	m	2/12	33800	9.5	34	yes	no	n.d.	46,XY,t(1;8;22)(p13;q22;q13)[14]/46,XY[1]	NR	no
KMT2A-r PDX #1	F	7	585	8.3	84	no	yes	n.d.	46,XX,t(9;11)(p22;q23)[8]/50,XX,idem,+3,+8,+18,+19[15]	CCR	no
KMT2A-r PDX #2	m	16	69.7	10.7	93	no	no	NRAS mutation	42~44,XY,t(6;11)(q27;q23)[cp2]/51,idem,+X,+der(6)t(6;11)(q27;q23),+8,+19,+21[5]	NR	no

Supplemental Table 4: Enrichment scores from the shRNA-based positive selection screen

Gene ID	log_2fold change	p.value	FDR	Gene ID	log_2fold change	p.value	FDR
Podxl	18,211	0,003266	0,692389	Tdg	-0,61991	0,51773	0,978994
Reep3	13,431	0,0091298	0,74172	Fam129b	-0,48297	0,53076	0,978994
Lpp	13,446	0,010496	0,74172	Slc38a9	-0,28405	0,53416	0,978994
E2f3	19,416	0,017347	0,744949	Acvr2a	-0,02331	0,53563	0,978994
Fzd5	18,417	0,021825	0,744949	Mknk2	-0,41859	0,54057	0,978994
Unc13b	11,016	0,022882	0,744949	Zswim4	-0,28989	0,54357	0,978994
Phc2	19,856	0,028716	0,744949	Otub2	-0,46519	0,55007	0,978994
Rnf144b	12,311	0,030172	0,744949	Arid3b	-0,70642	0,55106	0,978994
Arid3a	10,512	0,03808	0,744949	Ren	-0,23496	0,5538	0,978994
Map3k3	10,512	0,040254	0,744949	Gas2l1	-0,4527	0,55618	0,978994
Mef2c	0,79338	0,043784	0,744949	Fgfr1	0,13884	0,55941	0,978994
Bmf	0,65678	0,046188	0,744949	Plb1	0,21637	0,5625	0,978994
Cdr2l	14,542	0,047075	0,744949	Tmem	0,17315	0,58004	0,978994
Rbm38	0,30738	0,053767	0,744949	Accn2	-0,35256	0,58119	0,978994
Slc8a2	0,98054	0,057307	0,744949	Dapk1	-0,37717	0,58309	0,978994
Ptpro	-0,27504	0,060009	0,744949	Klf13	-0,22224	0,59137	0,978994
Mgat4a	0,79538	0,061575	0,744949	Ganc	-0,64927	0,59447	0,978994
Trim71	14,452	0,06325	0,744949	Pik3ip1	-0,09572	0,59794	0,978994
Acer3	0,32946	0,073492	0,800053	Neu1	-0,15549	0,60369	0,978994
AB124611	10,131	0,075477	0,800053	Cpeb3	0,090764	0,60671	0,978994
Setd7	0,3349	0,084332	0,812389	Tet2	-0,06904	0,60934	0,978994
Atp13a3	0,30916	0,086028	0,812389	Rit1	0,012464	0,6291	0,978994
1700025G04Rik	12,827	0,088281	0,812389	Tnfrsf1b	-0,60858	0,63755	0,978994
Abl2	0,64403	0,093686	0,812389	Tmem26	-0,34392	0,63984	0,978994
Gcnt1	0,82238	0,095801	0,812389	Bach1	-0,21152	0,65013	0,978994
Il13	0,60133	0,11553	0,902635	Arhgef1	-0,61972	0,65849	0,978994
Rhot2	11,383	0,11607	0,902635	Sh2b3	-0,72887	0,66269	0,978994
Ctdsp2	0,20944	0,11922	0,902635	Trib2	-0,7399	0,66931	0,978994
Abhd3	0,70079	0,13018	0,937048	Slco2b1	-0,53728	0,67162	0,978994
Foxn3	0,38527	0,13524	0,937048	Celsr2	-0,49381	0,67594	0,978994
Zfp697	0,60179	0,13974	0,937048	Bcat1	-0,69375	0,6822	0,978994
Tnfaip8l3	0,32358	0,15138	0,937048	Npl	-0,79773	0,68688	0,978994
Rufy3	0,62091	0,15338	0,937048	Vps4b	-0,13009	0,68758	0,978994
pGL2	0,78786	0,15853	0,937048	Tmod2	-0,92995	0,68873	0,978994
Ankrd29	0,64589	0,15892	0,937048	Coro1c	-0,78896	0,69119	0,978994
Apaf1	0,22716	0,16527	0,937048	Adam9	-0,11693	0,6954	0,978994
Itga7	-0,49822	0,16535	0,937048	Mapk14	-0,6026	0,69766	0,978994
Dusp3	0,80461	0,16796	0,937048	Mknk1	-0,26853	0,69821	0,978994
Mtus1	0,68293	0,18136	0,978994	Acvr2b	-0,86558	0,70004	0,978994
Dram2	0,49792	0,19822	0,978994	Trps1	-0,74998	0,70081	0,978994
Prdm1	-0,43376	0,20856	0,978994	Wipf2	0,11111	0,70418	0,978994

Mycl1	0,43842	0,22258	0,978994	Traf6	-0,38773	0,70536	0,978994
Syn2	0,61753	0,22503	0,978994	Irf4	-0,29991	0,70783	0,978994
Tmem87b	0,55059	0,23518	0,978994	Abhd6	-0,12295	0,71021	0,978994
Tbc1d14	0,2559	0,23784	0,978994	Snx18	-0,88071	0,71383	0,978994
Lactb	0,40593	0,24138	0,978994	Mcl1	-0,92353	0,7223	0,978994
Actr10	0,6169	0,24384	0,978994	Clic4	-10,906	0,72821	0,978994
Socs4	0,49086	0,2459	0,978994	Sgpl1	-0,82952	0,73709	0,978994
Rap1gap2	-0,11252	0,25879	0,978994	Baz2a	-0,72397	0,7395	0,978994
Tlr8	0,45459	0,26193	0,978994	St8sia4	-0,89706	0,74422	0,978994
Synj2bp	-0,7179	0,26485	0,978994	4930506M07Rik	-0,19725	0,74764	0,978994
Myo1e	0,33647	0,27106	0,978994	Cyth1	-0,75454	0,75325	0,978994
Zfp191	-0,042509	0,27414	0,978994	Stard13	-0,66165	0,75402	0,978994
Rbm20	0,42573	0,27709	0,978994	Apc	-0,73266	0,75865	0,978994
Ap4e1	0,4165	0,27825	0,978994	Csnk2a1	-0,47077	0,76303	0,978994
Tgfbr1	0,34813	0,28528	0,978994	Slc26a6	-1,281	0,769	0,978994
Srd5a3	0,44488	0,28654	0,978994	Rhoq	-1,211	0,77629	0,978994
Slc25a24	0,34794	0,29272	0,978994	Tmem86a	-0,86469	0,788	0,978994
Ube2g1	0,368	0,29547	0,978994	Cpeb4	-0,28298	0,79291	0,978994
Map3k1	0,080211	0,29665	0,978994	Rab8b	-0,39113	0,7985	0,978994
Nrp2	0,36459	0,29716	0,978994	Vps36	-0,31183	0,80079	0,978994
Pou2f2	0,29057	0,29933	0,978994	Glipr1	-0,76585	0,80981	0,978994
Lipa	0,25547	0,30457	0,978994	Etv6	-0,29548	0,81128	0,978994
Dnajb5	-0,10121	0,31046	0,978994	Lin28b	-0,7023	0,81554	0,978994
Sash1	-0,34621	0,31667	0,978994	Limd1	-0,77919	0,82361	0,978994
Lbh	-0,26441	0,32523	0,978994	Slc38a1	-0,27681	0,8255	0,978994
Trp53inp1	-0,21259	0,33128	0,978994	Smarcd1	-15,139	0,82567	0,978994
Asb13	-0,078531	0,33426	0,978994	Slc16a6	-0,94919	0,82993	0,978994
Mllt4	-0,24686	0,33428	0,978994	Myo7a	-0,63746	0,84056	0,978994
Msr1	-0,46842	0,3402	0,978994	Il6ra	-0,68388	0,8427	0,978994
Pald1	0,25211	0,34725	0,978994	Klf3	-0,19003	0,84834	0,978994
Frmd4b	0,31737	0,3548	0,978994	Borcs6	-11,788	0,84872	0,978994
Zfp710	-0,55893	0,35822	0,978994	Qk	-0,71527	0,85115	0,978994
Rtcd1	0,20179	0,35836	0,978994	St6gal1	-0,31826	0,85178	0,978994
Smad2	-0,26605	0,36126	0,978994	Rab22a	-0,79094	0,85311	0,978994
Mob3b	0,25667	0,36238	0,978994	Tmem135	-11,746	0,85781	0,978994
Map2k7	-0,50981	0,36447	0,978994	Fam65b	-0,56516	0,86327	0,978994
Ccr7	0,13359	0,36734	0,978994	Cgn	-13,818	0,86705	0,978994
Mllt10	0,014767	0,37345	0,978994	Fmn1	-0,2668	0,87236	0,978994
Rora	-0,27941	0,37913	0,978994	Olfml2a	-0,60646	0,87556	0,978994
Ncor2	0,1767	0,38154	0,978994	Gpc4	-0,7572	0,87726	0,978994
Lrrk2	0,094665	0,38844	0,978994	Mapk12	-11,806	0,87834	0,978994
Zswim6	-0,14512	0,3916	0,978994	Arrdc4	-0,76514	0,88483	0,978994
Psmb8	-0,31479	0,39451	0,978994	Ppp2ca	-0,68708	0,88644	0,978994
Cdk19	-0,58488	0,39729	0,978994	Trim7	-13,032	0,88796	0,978994
Slc16a10	-0,48462	0,4005	0,978994	Anapc16	-14,396	0,89237	0,978994

Nt5dc1	0,03504	0,40385	0,978994	Slc46a3	-0,95053	0,89565	0,978994
Bmpr2	0,23971	0,42228	0,978994	Pi4k2a	-1,07	0,89857	0,978994
Ank	-0,024537	0,42976	0,978994	Rassf3	-13,508	0,90049	0,978994
Bcl2l12	0,21234	0,43416	0,978994	Klhl24	-0,49806	0,90619	0,980169
Abtb1	-0,17867	0,44033	0,978994	Sept11	-14,237	0,91479	0,984444
Maf	0,25079	0,44511	0,978994	Dus1l	-1,315	0,92243	0,984962
Sertad3	-0,32769	0,4597	0,978994	Baiap2	-10,806	0,92456	0,984962
Atxn1l	-0,36812	0,46569	0,978994	Plekhm3	-0,52546	0,93347	0,986029
pGL3-Luc	-0,059947	0,48111	0,978994	Daam2	-17,783	0,94205	0,986029
Dusp7	-0,13643	0,48166	0,978994	Dazap2	-0,80727	0,9421	0,986029
Mfsd7c	-0,31089	0,48186	0,978994	Ttc7	-13,897	0,94417	0,986029
Tab2	-0,44637	0,48491	0,978994	Homez	-10,914	0,95449	0,987826
1700017B05Rik	-0,1604	0,48626	0,978994	Ppm1f	-1,284	0,95676	0,987826
Pctp	-0,22003	0,48808	0,978994	D17H6S53E	-13,874	0,96014	0,987826
Pik3c2b	-0,16198	0,49288	0,978994	Naif1	-21,675	0,96739	0,987826
E2f2	0,28522	0,49397	0,978994	Ipmk	-0,91672	0,97375	0,987826
Pdpk1	-0,017022	0,49701	0,978994	Snx30	-22,969	0,97385	0,987826
St5	0,20124	0,50954	0,978994	Rxra	-12,655	0,98608	0,994835
Srgap2	-0,39678	0,5125	0,978994	Kif1b	-16,994	0,99014	0,994835
Cecr6	0,097405	0,51548	0,978994	Ahrr	-19,762	0,99713	0,997133

Supplemental Table 5: GSEA results of global gene expression profiling after overexpression of miR-125b in *Gata1s*-FLCs

Hallmark gene sets [38]

#	Gene set	NES	NOM p	FDR q
1	HALLMARK_OXIDATIVE_PHOSPHORYLATION	2,292	0,000	0,000
2	HALLMARK_MYC_TARGETS_V1	2,279	0,000	0,000
3	HALLMARK_MYC_TARGETS_V2	1,916	0,000	0,000
4	HALLMARK_DNA_REPAIR	1,679	0,000	0,004
5	HALLMARK_E2F_TARGETS	1,591	0,000	0,009
6	HALLMARK_FATTY_ACID_METABOLISM	1,392	0,009	0,042
7	HALLMARK_REACTIVE_OXYGEN_SPECIES_PATHWAY	1,347	0,040	0,058
8	HALLMARK_UV_RESPONSE_UP	1,324	0,000	0,068
9	HALLMARK_ADIPOGENESIS	1,303	0,006	0,072
10	HALLMARK_MTORC1_SIGNALING	1,251	0,025	0,104
11	HALLMARK_KRAS_SIGNALING_DN	-1,450	0,001	0,148
12	HALLMARK_MITOTIC_SPINDLE	-1,317	0,011	0,394
13	HALLMARK_HEDGEHOG_SIGNALING	-1,285	0,091	0,382
14	HALLMARK_HEME_METABOLISM	-1,231	0,054	0,514
15	HALLMARK_TNFA_SIGNALING_VIA_NFKB	-1,222	0,050	0,451

StemCell and matured lineages genesets [7]

#	Gene set	NES	NOM p	FDR
1	WONG_EMBRYONIC_STEM_CELL_CORE	2,050	0,000	0,000
2	EZH2-KO IN ETP_UP	1,749	0,000	0,013
3	EZH2-KO IN ETP_IN_VIVO_UP	1,673	0,000	0,021
4	BHATTACHARYA_EMBRYONIC_STEM_CELL	1,633	0,000	0,027
5	ES_MYC_MODULE	1,585	0,000	0,035
6	LU_EZH2_TARGETS_UP	1,522	0,000	0,050
7	GEORGOPOLOUS_MYELOID DIFFERENTIATION	1,424	0,000	0,101
8	LAURENTI_CMP	1,349	0,000	0,165
9	LAURENTI_GMP	1,320	0,000	0,185
10	KUSTIKOVA TOP200_DOWN_EVI1	1,303	0,010	0,187
11	GEORGOPOLOUS_GMP VS ALL OTHER +CD33	1,300	0,024	0,174
12	ROSS_AML_WITH_MLL_FUSIONS	1,276	0,062	0,191
13	REGEV_G1-S_CORE SET	1,273	0,090	0,180
14	EBERT_HUMAN_MYELOID	1,263	0,012	0,182
15	KLUSMANN_ARRAYSTAR_MONO	1,259	0,058	0,175
16	HIDALGO_EZH1-KO IN HSC_UP	1,250	0,034	0,176
17	LAURENTI_MEP	1,235	0,000	0,188
18	KLUSMANN_NCODE_CD34	1,222	0,040	0,198
19	KLUSMANN_ARRAYSTAR_ERYTHROID	1,080	0,211	0,405
20	GOODELL_DNMT3 TARGETS	-1,594	0,000	0,062
21	IWAMA_EZH2-KO IN HSC_FL_UP	-1,476	0,000	0,186

22	EPPERT_LSC-R_EXTENDED	-1,445	0,009	0,191
23	EBERT_HUMAN_LYMPHOID	-1,421	0,017	0,194
24	EBERT_HUMAN_TCELLS	-1,418	0,014	0,161
25	KLUSMANN_NCODE_GRANULOCYTES	-1,330	0,015	0,379
26	EPPERT_LSC-R	-1,323	0,083	0,347
27	KUSTIKOVA TOP250_UP_EVI1	-1,289	0,010	0,438
28	KLUSMANN_NCODE_MEGAKARYOCYTIC	-1,267	0,042	0,492
29	ROSSI_T-CELLS	-1,261	0,047	0,473
30	FISCHER_DOWN IN RC	-1,246	0,080	0,499
31	KONDO_EZH2_TARGETS	-1,240	0,045	0,484
32	LAURENTI_MLP	-1,235	0,046	0,467
33	LU_EZH2_TARGETS_DN	-1,215	0,032	0,523
34	LAURENTI_HSC1 AND HSC2	-1,08	0,273	0,614

ML-DS signature genesets [7]

#	Gene set	NES	NOM p	FDR q
1	ML-DS TOP600 UP.GRP	1,899	0,000	0,000
2	ML-DS TOP500 UP.GRP	1,847	0,000	0,000
3	ML-DS TOP400 UP.GRP	1,842	0,000	0,000
4	ML-DS TOP250 UP.GRP	1,772	0,000	0,000
5	ML-DS TOP300_UP GENE.GRP	1,760	0,000	0,000
6	ML-DS TOP100_UP GENE.GRP	1,641	0,000	0,000
7	ML-DS TOP100_DOWN GENE.GRP	1,043	0,347	0,278
8	ML-DS TOP300_DOWN GENE.GRP	-1,246	0,049	0,227

Supplemental Table 6: List of shRNA targeting *ARID3A*/*Arid3a*

Mouse	**Sequence**
shArid3a #1	CTAGGAAGAATCTATCTGTATATAGTGAAGCCACAGATGTATATACAGATAGATTCTTCCTAA
shArid3a #2	AAAGAATCTATCTGTATATCTATAGTGAAGCCACAGATGTATAGATATACAGATAGATTCTTC
shArid3a #3	ACCCAAGATCAAGAAAGAGGAATAGTGAAGCCACAGATGTATTCCTCTTTCTTGATCTTGGGC

Human	**Sequence**
shARID3A #1	CAAGGATATCTATATATCTATATAGTGAAGCCACAGATGTATATAGATATATAGATATCCTTT
shARID3A #2	AGCCGATCCTGTTTACCTCATATAGTGAAGCCACAGATGTATATGAGGTAAACAGGATCGGCC
shARID3A #3	ATGGATGACTTGTTCAGCTTCATAGTGAAGCCACAGATGTATGAAGCTGAACAAGTCATCCAG

Non-targeting	**Sequence**
shLUC	CCAGGATTACAAGATTCAAAGTTAGTGAAGCCACAGATGTAACTTTGAATCTTGTAATCCTGA

Supplemental Table 8: Pairwise analysis of LC-MS/MS

Protein	log2FC (ARID3A/Control)	log_2pvalue
SMAD2	7,62	4,159926
P4HA1	6,01	3,867153
ARID3B	3,73	3,555343
TRIM21	5,36	3,488007
RBM15	4,82	3,466823
ARID3A	9,33	3,465567
SERPINH1	5,12	3,011139
SRRM2	5,48	2,736189
DACH1	8,93	2,718777
P4HB	6,49	2,636633
PCM1	5,85	2,634229
DHX15	4,05	2,5961
RNPS1	2,55	2,382591
MIB1	4,96	2,362444
COL1A1	8,94	2,196879
HSPA8	2,33	2,160015
RPL3	3,06	2,074202
NUMA1	2,93	1,990553
SSR4	2,6	1,796137
HADHA	2,75	1,730748
CCT7	4,21	1,723534
XRCC5	4,44	1,579291
PML	7,3	1,567755
LRRC59	4,21	1,539919
KPNB1	3,11	1,455751
RAN	3,59	1,349624
DLST	4,94	1,340969
PKM	3,7	1,179455
XRCC6	4,12	1,17568
VDAC1	2,56	0,860005
SSBP1	2,67	0,742064
ENO1	3,45	0,592388
A2ML1	2,64	0,489387
EEF2	2,29	0,390247
VCP	2,28	0,309687
GAPDH	2,36	0,217776
GSTP1	2,78	0,124319

Supplemental Table 9: GSEA results of global gene expression profiling after overexpression of *ARID3A* in CMK

Hallmark gene sets[38]

#	Gene set	NES	NOM p	FDR q
1	HALLMARK_TGF_BETA_SIGNALING	1,478	0,011	0,105
2	HALLMARK_MYOGENESIS	1,416	0,003	0,146
3	HALLMARK_TNFA_SIGNALING_VIA_NFKB	1,357	0,011	0,232
4	HALLMARK_P53_PATHWAY	1,330	0,020	0,249
5	HALLMARK_KRAS_SIGNALING_DN	1,280	0,035	0,376
6	HALLMARK_E2F_TARGETS	-1,636	0,000	0,017
7	HALLMARK_MYC_TARGETS_V1	-1,625	0,000	0,010
8	HALLMARK_UNFOLDED_PROTEIN_RESPONSE	-1,301	0,023	0,181
9	HALLMARK_MYC_TARGETS_V2	-1,140	0,188	0,494
10	HALLMARK_G2M_CHECKPOINT	-1,074	0,207	0,353

StemCell and matured lineages genesets[7]

#	Gene set	NES	NOM p	FDR
1	KLUSMANN_ARRAYSTAR_MEGA	1,584	0,000	0,029
2	EZH2-KO_IN ETP_H3K27ME3_DOWN	1,580	0,000	0,015
3	LAURENTI_MLP	1,496	0,000	0,071
4	KLUSMANN_NCODE_NKC	1,471	0,006	0,089
5	KLUSMANN_NCODE_MEGAKARYOCYTIC	1,356	0,005	0,427
6	IWAMA_EZH2-KO IN HSC_BM_UP	1,324	0,024	0,519
7	KUSTIKOVA TOP400_UP_EVI1	1,317	0,006	0,489
8	KLUSMANN_ARRAYSTAR_HSPC_CB VS ALL_TOP200	1,308	0,037	0,473
9	GOODELL_NK	1,287	0,095	0,528
10	GOODELL_NAIVE	1,283	0,115	0,500
11	KLUSMANN_NCODE_GRANULOCYTES	1,276	0,037	0,489
12	KLUSMANN_ARRAYSTAR_GRANULOCYTES	1,264	0,036	0,509
13	LAURENTI_HSC1 VS HSC2	1,004	0,482	0,719
14	REGEV_G1-S_CORE SET	-1,748	0,000	0,005
15	LAURENTI_MEP	-1,744	0,000	0,003
16	ROSS_AML_OF_FAB_M7_TYPE	-1,700	0,000	0,004
17	KAMMINGA_EZH2_TARGETS	-1,519	0,000	0,052
18	JAATINEN_HEMATOPOIETIC_STEM_CELL_UP	-1,488	0,000	0,061
19	EBERT_HUMAN_CD34	-1,463	0,000	0,066
20	WONG_EMBRYONIC_STEM_CELL_CORE	-1,427	0,000	0,079
21	EBERT_HUMAN HSC	-1,357	0,012	0,124
22	KLUSMANN_ARRAYSTAR_MONO	-1,343	0,031	0,121
23	KUSTIKOVA TOP200_DOWN_EVI1	-1,326	0,026	0,126
24	NOLAN_IFPC	-1,266	0,097	0,175
25	FISCHER_DOWN IN SAA	-1,240	0,038	0,195
26	FISCHER_SAA_RC_DOWN	-1,232	0,021	0,190

27	SUZ12_DOWN	-1,213	0,000	0,203
28	LAURENTI_CMP	-1,208	0,029	0,197

ML-DS signature genesets[7]

#	Gene set	NES	NOM p	FDR q
1	ML-DS TOP250 DOWN.GRP	1,374	0,007	0,044
2	ML-DS TOP400 DOWN.GRP	1,369	0,006	0,024
3	ML-DS TOP600 DOWN.GRP	1,352	0,000	0,020
4	ML-DS TOP750 DOWN.GRP	1,341	0,000	0,017
5	ML-DS TOP500 DOWN.GRP	1,337	0,000	0,015
6	ML-DS TOP300_DOWN GENE.GRP	1,319	0,022	0,017
7	ML-DS TOP100_DOWN GENE.GRP	1,270	0,084	0,030
8	ML-DS TOP400 UP.GRP	-1,734	0,000	0,000
9	ML-DS TOP300_UP GENE.GRP	-1,670	0,000	0,000
10	ML-DS TOP250 UP.GRP	-1,658	0,000	0,000
11	ML-DS TOP500 UP.GRP	-1,642	0,000	0,000
12	ML-DS TOP100_UP GENE.GRP	-1,632	0,000	0,000
13	ML-DS TOP600 UP.GRP	-1,591	0,000	0,000

Supplemental Table 10: Multivariate cox regression analysis

Variable	EFS		OS	
	HR (95% CI)	P-value	HR (95% CI)	P-value
ARID3A	0.68 (0.50 - 0.94)	0.018	0.66 (0.45 - 0.97)	0.033
Dataset	1.09 (0.79 - 1.51)	0.605	1.51 (1.05 - 2.16)	0.025
Risk group favourable	0.43 (0.32 - 0.58)	<0.001	0.41 (0.29 - 0.60)	<0.001
Risk group adverse	1.24 (0.92 - 1.67)	0.16	1.56 (1.13 - 2.14)	0.007
Gender	1.18 (0.93 - 1.49)	0.165	1.29 (0.99 - 1.67)	0.058
Age ≥ 60 y	2.19 (1.55 - 3.11)	<0.001	2.76 (1.91 - 3.97)	<0.001
WBC ≥ 20 x 10^9/L	1.61 (1.23 - 2.11)	<0.001	1.36 (1.01 - 1.83)	0.041

Supplemental Figures

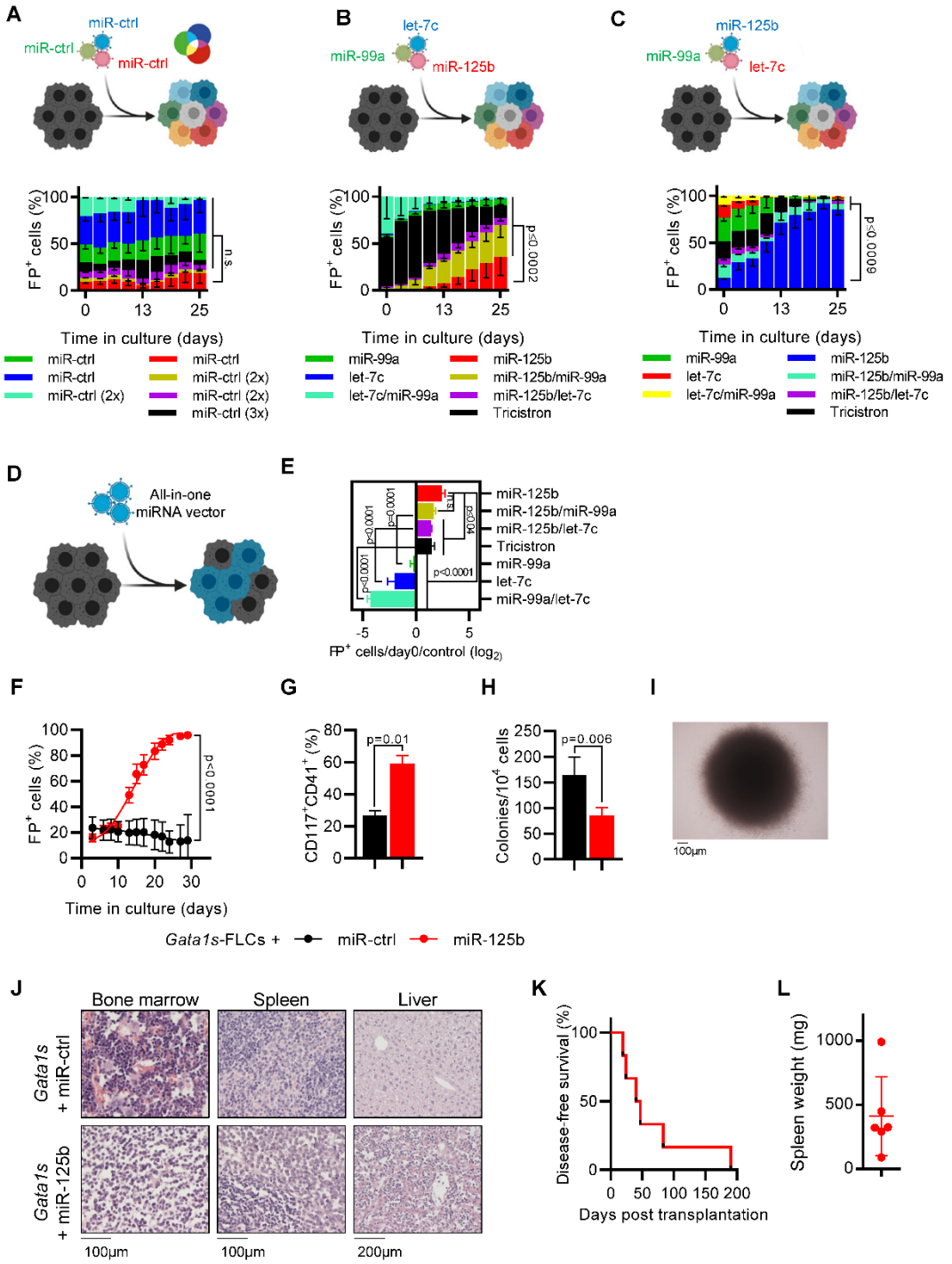

Supplemental Figure 1. Validation of miR-125b as the dominant oncogenic member of the miR-99a~125b tricistrons synergizing with *Gata1s*.

(A-C, top) Schematic of Red-Green-Blue-based lentiviral co-transduction[39]. Co-transduction with different fluorescent protein (FP) reporters allows for multicolor tracking and competition analysis between independent populations.

(A, bottom) Percentage of *Gata1s*-FLCs transduced with different miR-control (marked by dTomato, mTagBFP2 or GFP) permutations (n=6, one-way ANOVA on day 0-normalized fold changes).

(B, bottom) Percentage of *Gata1s*-FLCs transduced with different miRNA permutations (marked by dTomato [miR-125b], mTagBFP2 [let-7c] and GFP [miR-99a]) (n=4, one-way ANOVA on day 0-normalized fold changes).

(C, bottom) Percentage of *Gata1s*-FLCs transduced with different miRNA permutations (marked by dTomato [let-7c], mTagBFP2 [miR-125b] and GFP [miR-99a]) (n=6, one-way ANOVA on day 0-normalized fold changes). Note alternating miRNA-fluorescent color combinations compared to B.
(D-E) Schematic of classical growth competition assays, where *Gata1s*-FLCs were transduced with single lentiviral vectors encoding different permutations of miRNAs of the miR-99~125b cluster (D). Data are depicted as percentage of miRNA-transduced *Gata1s*-FLCs on day 12 of differentiation, normalized to day 0 (n=3, one-way ANOVA) (E).
(F) Percentage of miR-ctrl- or miR-125b-transduced *Gata1s*-FLCs (n=6, unpaired t-test on day 29).
(G) Bar graph showing the percentage of megakaryocytic progenitors ($CD117^+CD41^+$) after 6 days of differentiation. The depicted cells are *Gata1s*-FLCs transduced with miR-125b or miR-ctrl (n=3, paired t-test).
(H) Bar graph showing colony counts from miR-125b- or miR-Control- transduced *Gata1s*-FLCs in methylcellulose-based CFU-assays with complete cytokine conditions (n=4, unpaired t-test).
(I) Representative blast-like colony from one of n=4 independent methylcellulose-based CFU-assays using miR-125b-transduced *Gata1s*-FLCs and minimal (Thpo 20ng/ml) cytokine conditions. Scale is indicated.
(J) Representative micrographs of bone marrow (sternum), spleen and liver samples from mice transplanted with miR-ctrl (top) or miR-125b (bottom) transduced *Gata1s*-FLCs. The *Gata1s*-miR-125b condition shows bone marrow with a monotonous blastoid infiltrate with an absence of megakaryocytes, and spleen and liver blastoid infiltrates. Magnifications: 200x (liver), 400x (bone marrow and spleen).
(K-L) Kaplan-Meier survival curve (K) and spleen weights (L) of secondary recipients transplanted with miR-125b-transduced *Gata1s*-FLCs (25% of bone marrow of primary leukemic recipients) (n=6).
Data are presented as mean ± SD. n.s., not significant, FP^+= fluorescent protein-positive.

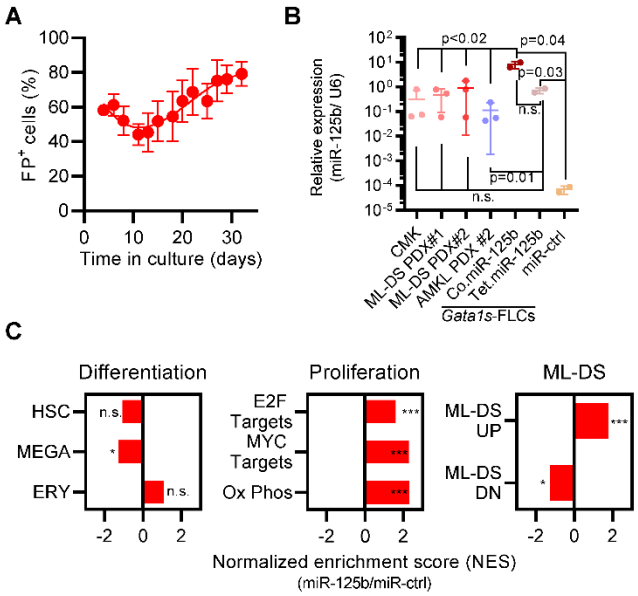

Supplemental Figure 2. Sustained miR-125b expression induces an ML-DS-like gene expression signature in *Gata1s*-FLCs.

(A) Percentage of *Gata1s*-FLCs containing the miR-125b-mimic shRNA pool over time (n=6). Data are presented as mean ± SD.

(B) Expression of miR-125b relative to U6, as measured by RT-qPCR (TaqMan) in CMK cells (n=3), ML-DS and AMKL PDXs (n=3), and *Gata1s*-FLCs transduced with miR-ctrl, constitutive miR-125b (Co.miR-125b) and inducible miR-125b (Tet.miR-125b) 72 hours after transduction or 2 days after doxycycline induction (n=2). Data are presented as mean ± SD (unpaired t-test).

(C) Bar graphs showing normalized enrichment scores from GSEA on hematopoietic differentiation- and cell proliferation-related gene sets. *Gata1s*-FLCs overexpressing miR-125 were compared to *Gata1s*-FLCs overexpressing miR-ctrl. In both cases, cells were taken after 10 days of doxycycline induction. * p<0.05; ** p<0.01; *** p<0.001.

n.s., not significant, FP+= fluorescent protein-positive.

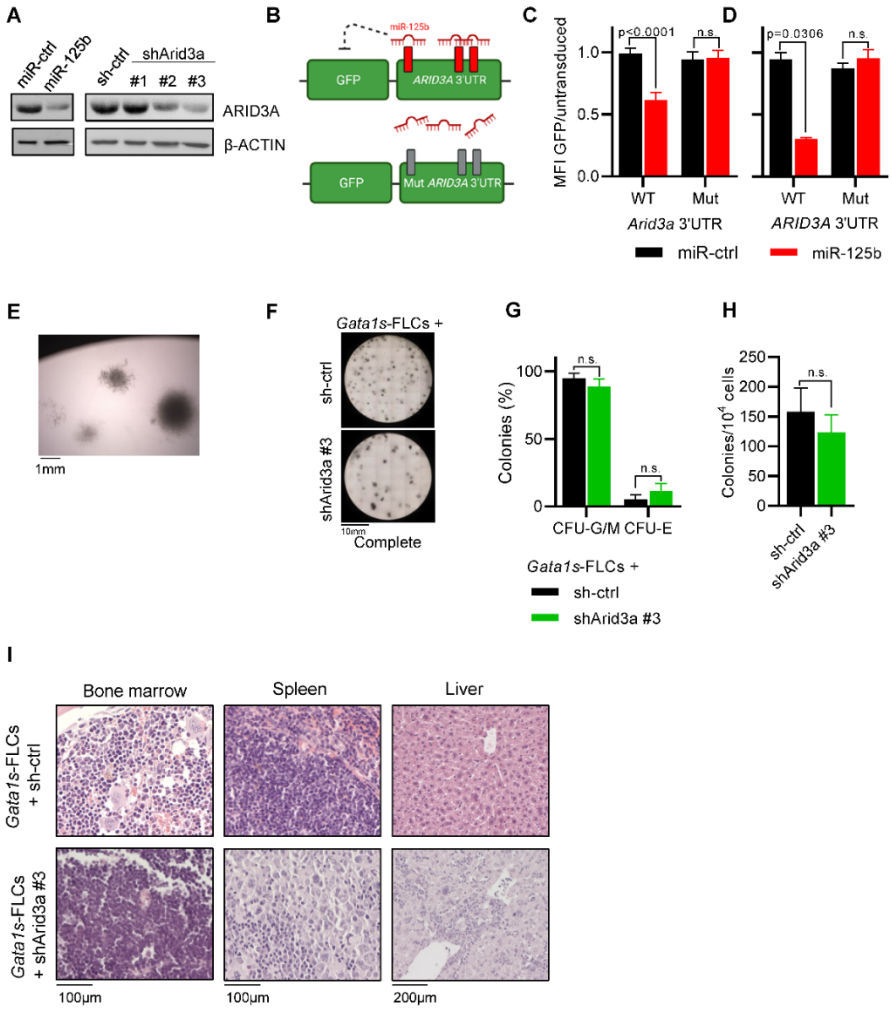

Supplemental Figure 3. Verification of *Arid3a* as the main target of miR-125b synergizing with *Gata1s*.

(A) Western Blot showing ARID3A protein levels in *Gata1s*-FLCs 4 days after transduction with miR-125b or shRNAs targeting *Arid3a*, as well as their respective controls. Position of ARID3A (63kDa) and β-Actin (43kDa) is indicated.

(B) Experimental design of *ARID3A* 3'UTR assays. miR-125b can bind to the 3'UTR and impair GFP expression only when the miR-125b-binding sites are intact.

(C and D) GFP Mean fluorescence intensity of HEL cells expressing wildtype or a mutated 3'UTR of *Arid3a* (B) or *ARID3A* (C) after transduction with miR-125b or miR-Control. MFI is normalized to untransduced cells. (n=12 and n=3, respectively; unpaired t-test).

(E) Representative megakaryocytic-like colony from one of n=3 independent methylcellulose-based CFU-assays after plating *Gata1s*-FLCs transduced with shArid3a #3 in minimal (Thpo 20ng/ml) cytokine conditions.

(F-H) (F) Representative image, (G) classification of colonies and (H) number of formed colonies after plating transduced (sh-ctrl [black] or shArid3a #3 ([green]) *Gata1s*-FLCs in methylcellulose-based CFU assays under complete cytokine conditions (n=3, two-way ANOVA (G) and unpaired t-test (H)). CFU-G/M: granulocytic (CFU-G), monocytic (CFU-M) and granulocytic/monocytic (CFU-GM); CFU-E: erythroid.

(I) Representative micrographs of bone marrow (sternum), spleen and liver from mice transplanted with sh-ctrl (top) or shArid3a #3 (bottom) transduced *Gata1s*-FLCs. The *Gata1s*-shArid3a condition shows bone marrow with a monotonous blastoid infiltrate, and spleen and liver samples enriched for megakaryoblastic-like infiltrates. Magnifications: 200x (liver), 400x (bone marrow and spleen).

All data are presented as mean ± SD. n.s., not significant.

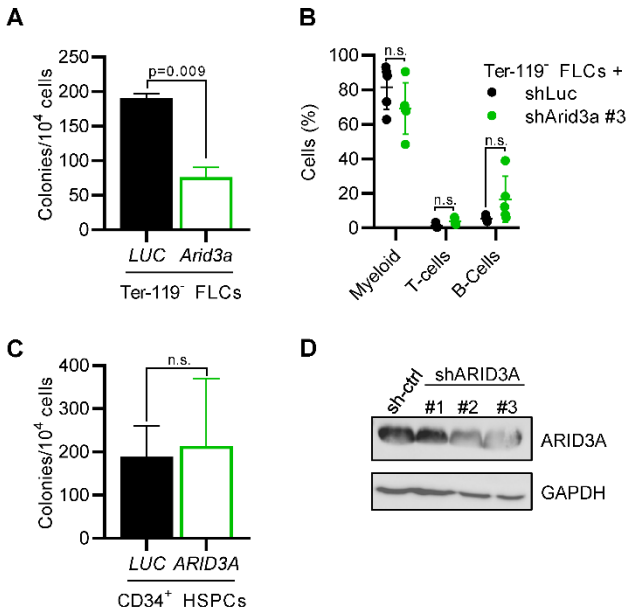

Supplemental Figure 4. Number of CFUs formed in methylcellulose-based assays and knockdown efficiency of shRNAs against *ARID3A*.

(A) Number of colonies formed after plating transduced (*Arid3a* or *LUC* cDNA) murine FLCs in methylcellulose-based CFU assays under complete cytokine conditions (n=3, unpaired t-test).

(B) Bar graph showing the percentage of myeloid ($CD11b^+$), T-cells ($CD3e^+$) and B-cells ($B220^+$) in the BM of mice transplanted with Ter-119^- FLCs transduced with sh-ctrl (black) or shArid3a (green). $shRNA^+$ cells shown (n=5, unpaired t-test).

(C) Number of colonies formed after plating *ARID3A*- or *LUC*-expressing human adult PB $CD34^+$ HSPCs in methylcellulose-based CFU assays under complete cytokine conditions (n=3, unpaired t-test).

(D) Western Blot showing ARID3A protein levels in K562 4 days after transduction with shRNAs targeting *ARID3A*, as well as a non-targeting control (sh-ctrl). Position of ARID3A (63kDa) and GAPDH (37kDa) is indicated.

All data are presented as mean ± SD. n.s., not significant.

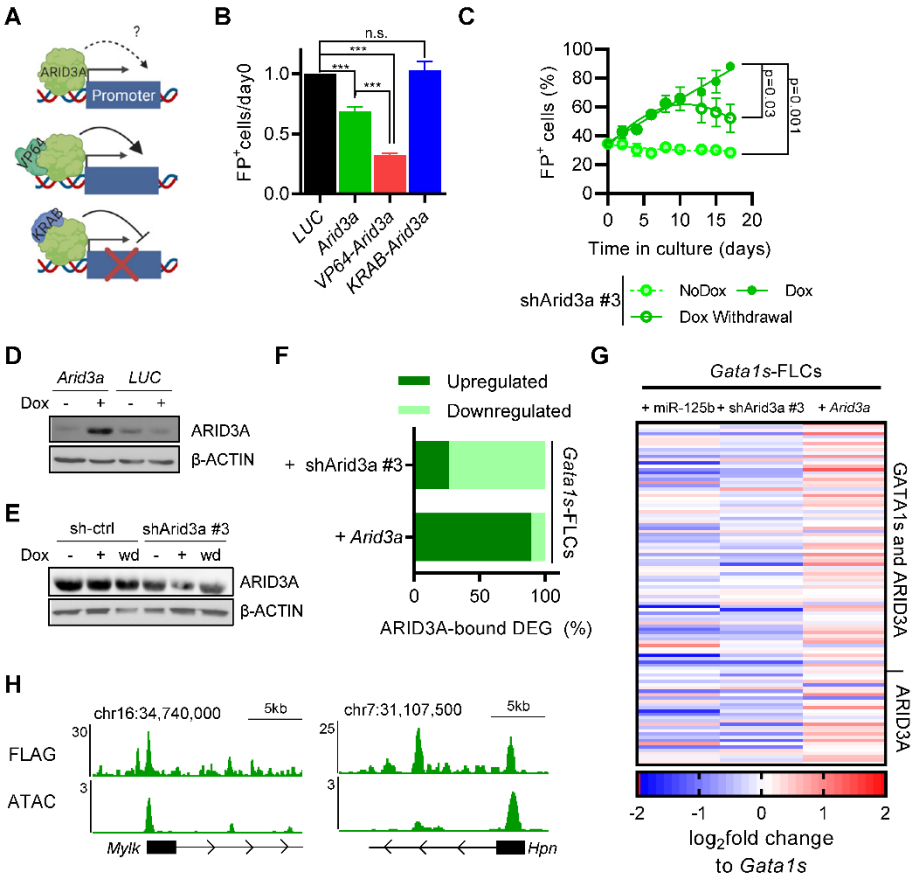

Supplemental Figure 5. ARID3A activates expression of genes involved in megakaryocytic differentiation.

(A-B) Schematic of setup to determine the role of ARID3A in gene transcription by fusing the VP64-activator or KRAB-inhibitor domains to its N-terminal domain (A) and normalized percentage (to *LUC* cDNA) of transduced (*Arid3a* (green), *VP64-Arid3a* (red) or *KRAB-Arid3a* (blue)) *Gata1s*-FLCs after 10 days in culture. n=3; *= p_{ANOVA}<0.05; ** = p_{ANOVA}<0.01; ***=p_{ANOVA}<0.001 (one-way ANOVA).

(C) Percentage of *Gata1s*-FLCs expressing doxycycline-regulated shArid3a #3 upon addition or removal of doxycycline (500ng/mL) (n=3, paired t-test). Data are presented as mean ± SD.

(D and E) Western Blot showing ARID3A protein levels of *Gata1s*-FLCs 4 days after doxycycline-mediated induction of *Arid3a* (D) or shArid3a (E) expression (or its respective controls). Samples after doxycycline withdrawal (wd) were taken 2 days after removal of doxycycline. Position of ARID3A (63kDa) and β-ACTIN (43kDa) is indicated.

(F) Expression profile of differentially expressed genes (DEG) bound by ARID3A in *Gata1s*-FLCs after induction of *Arid3a* or shArid3a #3 (n=212 and n=329, respectively).

(G) Gene expression profile of genes involved in megakaryocytic differentiation upon modulation of *Arid3a* expression in *Gata1s*-FLCs. Data shown as log_2fold change to each respective control, binding by ARID3A or GATA1s and ARID3A is indicated (right).

(H) IGV snapshot showing occupancy (top) of megakaryocytic genes by ARID3A and associated open chromatin state (bottom). The tracks display coverage (RPKM) (left). Scale and chromosome location are shown (top).

FP^+= fluorescent protein-positive.

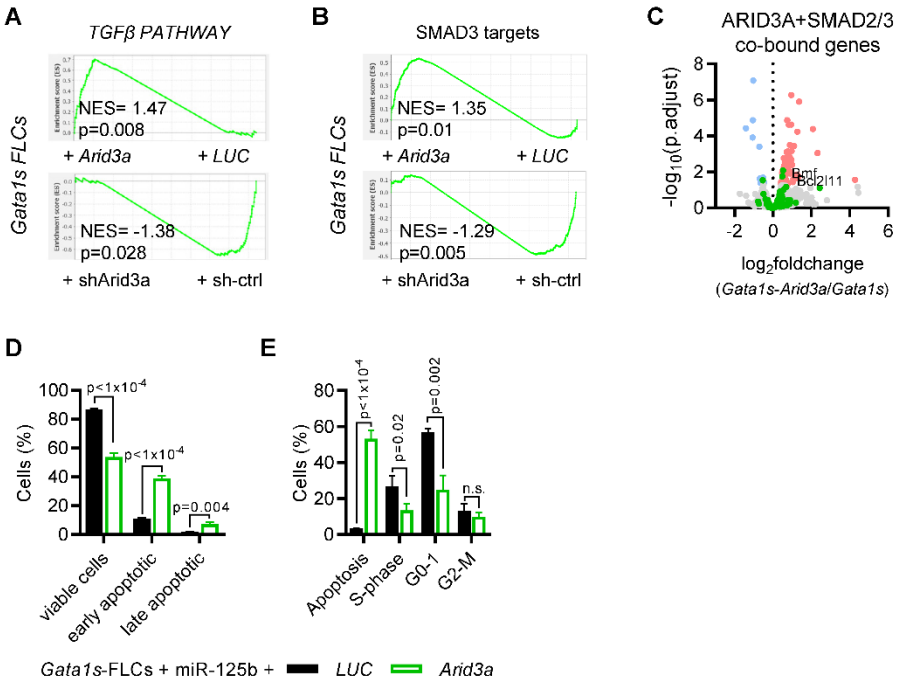

Supplemental Figure 6. ARID3A binds to SMAD2/3 activating TGFβ-mediated apoptosis and cell cycle arrest.

(A-B) GSEA enrichment plots showing the modulation of the TGFβ signaling pathway (A) and induction of SMAD3 targeted genes (B) upon *Arid3a* induction or repression in *Gata1s*-FLCs.

(C) Volcano plot showing differential expression of genes bound by ARID3A and SMAD2 and/or SMAD3[27] after doxycycline-induced *Arid3a* expression in *Gata1s*-FLCs. Genes involved in apoptosis and cell cycle arrest are highlighted in green; significantly downregulated and upregulated genes in blue and red, respectively.

(D) Percentage of viable, early and late apoptotic *Gata1s*-FLCs overexpressing miR-125b after 3 days of doxycycline induction of *Arid3a* expression as determined by Annexin-V assay. Viable cells: Annexin-V^-/$DAPI^-$; early apoptotic: Annexin-V^+/$DAPI^-$; late apoptotic: Annexin-V^+/$DAPI^+$ (n=3, unpaired t-test).

(E) Percentage of *Gata1s*-FLCs overexpressing miR-125b in apoptosis, S-phase, G0-1 and G2-M after 3 days of doxycycline induction of *Arid3a* expression as determined in BrDU-based cell cycle assay. Apoptosis: $BrdU^-$/$DAPI^-$; G0-1: $BrdU^-$/$DAPI^{low}$; S-Phase: $BrdU^+$/$DAPI^+$; G2-M: $BrdU^-$/ $DAPI^{high}$ (n=3 unpaired t-test).

Data are presented as mean ± SD. n.s., not significant.

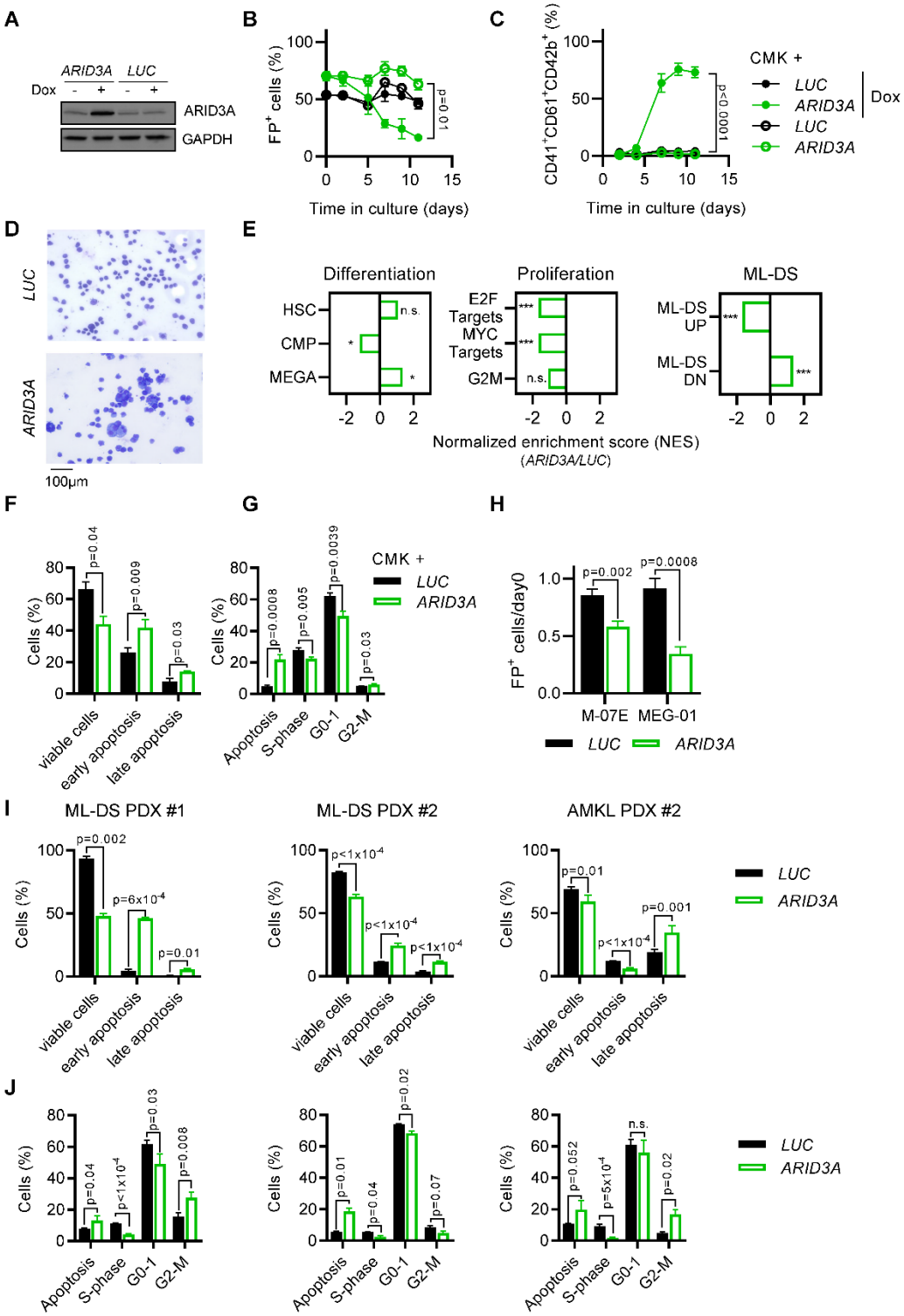

Supplemental Figure 7. Overexpression of *ARID3A* in the ML-DS cell line CMK restores differentiation potential and mediates cell cycle arrest and apoptosis.

(A) Western Blot showing ARID3A protein levels in CMK cells 4 days after doxycycline-mediated induction of *ARID3A* or *LUC* cDNA expression. Position of ARID3A (63kDa) and GAPDH (37kDa) is indicated.

(B-D) Percentage of fluorescent reporter positive (B) and percentage of mature megakaryocytic cells ($CD41^+CD61^+CD42b^+$) after doxycycline induction of CMK cells transduced with dox-inducible *ARID3A* or *LUC* cDNAs (C) (n=3, unpaired t-test, no differences between induced and non-induced control). Representative micrograph of n=3 experiments (D).

(E) Bar graphs showing normalized enrichment scores from GSEA of up- or downregulated gene sets involved in hematopoietic differentiation, cell proliferation and ML-DS progression. CMK overexpressing *ARID3A* were compared to CMK overexpressing *LUC* cDNA two days after doxycycline induction. *= p<0.05; ** = p<0.01; ***=p<0.001.

(F) Percentage of viable, early and late apoptotic CMK cells after 7 days of doxycycline induction of *ARID3A* expression as determined by Annexin-V assay. Viable cells: Annexin-V^-/$DAPI^-$; early apoptotic: Annexin-V^+/$DAPI^-$; late apoptotic: Annexin-V^+/$DAPI^+$ (n=3, unpaired t-test).

(G) Percentage of CMK cells in apoptosis, S-phase, G0-1 and G2-M after 7 days of doxycycline induction of *ARID3A* expression as determined in BrDU-based cell cycle assay. Apoptosis: $BrdU^-$/$7\text{-}AAD^-$; G0-1: $BrdU^-$/$7\text{-}AAD^{low}$; S-Phase: $BrdU^+$/$7\text{-}AAD^+$; G2-M: $BrdU^-$/$7\text{-}AAD^{high}$ (n=3, unpaired t-test).

(H) Normalized (to *LUC*) percentage of M-07E or MEG-01 cells expressing constitutively expressed *ARID3A* after 10 days in culture (n=3, unpaired t-test).

(I) Percentage of viable, early and late apoptotic ML-DS and AMKL PDXs after 2 days of doxycycline induction of *ARID3A* expression as determined by Annexin-V assay. Viable cells: Annexin-V^-/$DAPI^-$; early apoptotic: Annexin-V^+/$DAPI^-$; late apoptotic: Annexin-V^+/$DAPI^+$ (n=2-4, unpaired t-test).

(J) Percentage of ML-DS and AMKL PDXs in apoptosis, S-phase, G0-1 and G2-M after 2 days of doxycycline induction of *ARID3A* expression as determined in BrDU-based cell cycle assay. Apoptosis: $BrdU^-$/$DAPI^-$; G0-1: $BrdU^-$/$DAPI^{low}$; S-Phase: $BrdU^+$/$DAPI^+$; G2-M: $BrdU^-$/$DAPI^{high}$ (n=2-4, unpaired t-test).

All data are presented as mean ± SD. FP^+= fluorescent protein-positive.

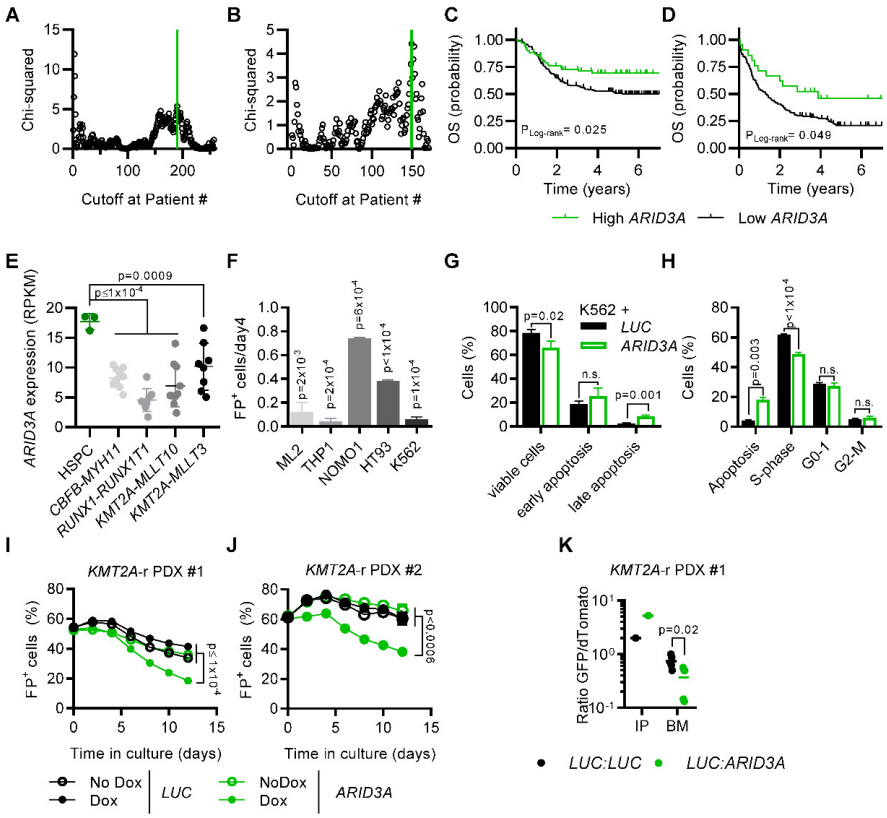

Supplemental Figure 8. ARID3A is a global tumor suppressor in AML

(A-B) Event-free survival (EFS) statistic (Chi-squared) as function of the cutoff point in the NCI-TARGET (A) and the TCGA (B) patient populations. The calculated optimum cutoff for EFS (green line, as determined by maximally selected rank statistics) – 12.0 and 12.3 normalized ARID3A reads, respectively – was used for both OS and EFS computations.

(C) Probability of overall survival (OS) in 258 pediatric AML patients[40] with high (green; >12.0 normalized reads) or low *ARID3A* expression (black; ≤12.0 normalized reads).

(D) Probability of overall survival (OS) in 171 adult AML patients[41] with high (green; >12.3 normalized reads) or low *ARID3A* expression (black; ≤12.3 normalized reads).

(E) *ARID3A* expression (RPKM) in sorted pediatric AML blasts of fetal CD34$^+$ HSPCs (n=3) and different non-AMKL subtypes: *CBFB-MYH11* (n=12*), RUNX1-RUNX1T1* (n=8), *KMT2A-MLLT10* (n=10) and *KMT2A-MLLT3* (n=8) (one-way ANOVA).

(F) Bar graph showing the percentage of *ARID3A*$^+$ cells after 7 days of induction with doxycycline, normalized to the *LUC* control (n=3, unpaired t-test compared to *LUC* control).

(G) Percentage of viable, early and late apoptotic K562 cells after 7 days of doxycycline induction of *ARID3A* expression as determined by Annexin-V assay. Viable cells: Annexin-V$^-$/DAPI$^-$; early apoptotic: Annexin-V$^+$/DAPI$^-$; late apoptotic: Annexin-V$^+$/DAPI$^+$ (n=3, unpaired t-test).

(H) Percentage of K562 cells in apoptosis, S-phase, G0-1 and G2-M after 7 days of doxycycline induction of *ARID3A* expression as determined in BrDU-based cell cycle assay. Apoptosis: BrdU$^-$/7-AAD$^-$; G0-1: BrdU$^-$/7-AAD^{low}; S-Phase: BrdU$^+$/7-AAD$^+$; G2-M: BrdU$^-$/7-AAD^{high} (n=3, unpaired t-test).

(I-J) *KMT2A*-rearranged (*KMT2A*-r) PDXs #1 and #2 were transduced with doxycycline-inducible *ARID3A* or *LUC* cDNA vectors. Percentage of fluorescent reporter positive cells after doxycycline induction of *KMT2A*-r PDX #1 (I) or *KMT2A*-r PDX #2 (J) (n=3, unpaired t-test).

(K) Ratio of GFP$^+$ to dTomato$^+$ cells in input cells (IP), and in the bone marrow (BM) of mice sacrificed 4-5 weeks after transplantation of *KMT2A*-r PDX #1 transduced with *ARID3A* (GFP$^+$) or a *LUC* control (GFP$^+$) and mixed 1:1 with *LUC* control-transduced blasts (dTomato$^+$) before transplantation (n=5, unpaired t-test).

All data are presented as mean ± SD. FP$^+$= fluorescent protein-positive.

Supplemental Information References

1. Gialesaki S, Mahnken AK, Schmid L, et al. GATA1s exerts developmental stage-specific effects in human hematopoiesis. *Haematologica*. 2018;103(8):e336-e340.
2. Labuhn M, Perkins K, Matzk S, et al. Mechanisms of Progression of Myeloid Preleukemia to Transformed Myeloid Leukemia in Children with Down Syndrome. *Cancer Cell*. 2019;36(2):123-138.e110.
3. Emmrich S, Rasche M, Schöning J, et al. miR-99a/100~125b tricistrons regulate hematopoietic stem and progenitor cell homeostasis by shifting the balance between TGFβ and Wnt signaling. *Genes & development*. 2014;28(8):858-874.
4. Klusmann JH, Li Z, Böhmer K, et al. miR-125b-2 is a potential oncomiR on human chromosome 21 in megakaryoblastic leukemia. *Genes Dev*. 2010;24(5):478-490.
5. Adams FF, Heckl D, Hoffmann T, et al. An optimized lentiviral vector system for conditional RNAi and efficient cloning of microRNA embedded short hairpin RNA libraries. *Biomaterials*. 2017;139:102-115.
6. Fellmann C, Zuber J, McJunkin K, et al. Functional identification of optimized RNAi triggers using a massively parallel sensor assay. *Mol Cell*. 2011;41(6):733-746.
7. Schwarzer A, Emmrich S, Schmidt F, et al. The non-coding RNA landscape of human hematopoiesis and leukemia. *Nat Commun*. 2017;8(1):218.
8. Li W, Xu H, Xiao T, et al. MAGeCK enables robust identification of essential genes from genome-scale CRISPR/Cas9 knockout screens. *Genome Biology*. 2014;15(12):554.
9. Wiśniewski JR, Zougman A, Nagaraj N, Mann M. Universal sample preparation method for proteome analysis. *Nature Methods*. 2009;6(5):359-362.
10. Consortium TU. UniProt: the universal protein knowledgebase in 2021. *Nucleic Acids Research*. 2020;49(D1):D480-D489.
11. Eng JK, McCormack AL, Yates JR. An approach to correlate tandem mass spectral data of peptides with amino acid sequences in a protein database. *Journal of the American Society for Mass Spectrometry*. 1994;5(11):976-989.
12. Labuhn M, Adams FF, Ng M, et al. Refined sgRNA efficacy prediction improves large- and small-scale CRISPR-Cas9 applications. *Nucleic Acids Res*. 2018;46(3):1375-1385.
13. Chen S, Zhou Y, Chen Y, Gu J. fastp: an ultra-fast all-in-one FASTQ preprocessor. *Bioinformatics*. 2018;34(17):i884-i890.
14. Spinozzi G, Tini V, Mincarelli L, Falini B, Martelli M. A comprehensive RNA-Seq pipeline includes meta-analysis, interactivity and automatic reporting; 2018.
15. Love MI, Huber W, Anders S. Moderated estimation of fold change and dispersion for RNA-seq data with DESeq2. *Genome Biology*. 2014;15(12):550.
16. Benjamini Y, Hochberg Y. Controlling the False Discovery Rate: A Practical and Powerful Approach to Multiple Testing. *Journal of the Royal Statistical Society: Series B (Methodological)*. 1995;57(1):289-300.
17. Subramanian A, Tamayo P, Mootha VK, et al. Gene set enrichment analysis: a knowledge-based approach for interpreting genome-wide expression profiles. *Proc Natl Acad Sci U S A*. 2005;102(43):15545-15550.
18. Aken BL, Achuthan P, Akanni W, et al. Ensembl 2017. *Nucleic Acids Res*. 2017;45(D1):D635-d642.
19. Skene PJ, Henikoff S. An efficient targeted nuclease strategy for high-resolution mapping of DNA binding sites. *Elife*. 2017;6.
20. Meers MP, Bryson TD, Henikoff JG, Henikoff S. Improved CUT&RUN chromatin profiling tools. *Elife*. 2019;8.
21. Bolger AM, Lohse M, Usadel B. Trimmomatic: a flexible trimmer for Illumina sequence data. *Bioinformatics*. 2014;30(15):2114-2120.

22. Zhu Q, Liu N, Orkin SH, Yuan G-C. CUT&RUNTools: a flexible pipeline for CUT&RUN processing and footprint analysis. *Genome Biology*. 2019;20(1):192.
23. Langmead B, Salzberg SL. Fast gapped-read alignment with Bowtie 2. *Nat Methods*. 2012;9(4):357-359.
24. Li H, Handsaker B, Wysoker A, et al. The Sequence Alignment/Map format and SAMtools. *Bioinformatics*. 2009;25(16):2078-2079.
25. Ramírez F, Ryan DP, Grüning B, et al. deepTools2: a next generation web server for deep-sequencing data analysis. *Nucleic Acids Res*. 2016;44(W1):W160-165.
26. Robinson JT, Thorvaldsdóttir H, Winckler W, et al. Integrative genomics viewer. *Nat Biotechnol*. 2011;29(1):24-26.
27. Meers MP, Tenenbaum D, Henikoff S. Peak calling by Sparse Enrichment Analysis for CUT&RUN chromatin profiling. *Epigenetics & Chromatin*. 2019;12(1):42.
28. Heinz S, Benner C, Spann N, et al. Simple combinations of lineage-determining transcription factors prime cis-regulatory elements required for macrophage and B cell identities. *Mol Cell*. 2010;38(4):576-589.
29. Kai Y, Andricovich J, Zeng Z, Zhu J, Tzatsos A, Peng W. Predicting CTCF-mediated chromatin interactions by integrating genomic and epigenomic features. *Nature Communications*. 2018;9(1):4221.
30. Buenrostro JD, Wu B, Chang HY, Greenleaf WJ. ATAC-seq: A Method for Assaying Chromatin Accessibility Genome-Wide. *Curr Protoc Mol Biol*. 2015;109:21.29.21-21.29.29.
31. Buenrostro JD, Giresi PG, Zaba LC, Chang HY, Greenleaf WJ. Transposition of native chromatin for fast and sensitive epigenomic profiling of open chromatin, DNA-binding proteins and nucleosome position. *Nature Methods*. 2013;10(12):1213-1218.
32. Jiang H, Lei R, Ding S-W, Zhu S. Skewer: a fast and accurate adapter trimmer for next-generation sequencing paired-end reads. *BMC Bioinformatics*. 2014;15(1):182.
33. Li H, Durbin R. Fast and accurate short read alignment with Burrows-Wheeler transform. *Bioinformatics*. 2009;25(14):1754-1760.
34. Kaplan EL, Meier P. Nonparametric Estimation from Incomplete Observations. *Journal of the American Statistical Association*. 1958;53(282):457-481.
35. Mantel N. Evaluation of survival data and two new rank order statistics arising in its consideration. *Cancer Chemother Rep*. 1966;50(3):163-170.
36. Leek JT, Johnson WE, Parker HS, Jaffe AE, Storey JD. The sva package for removing batch effects and other unwanted variation in high-throughput experiments. *Bioinformatics*. 2012;28(6):882-883.
37. Cox DR. Regression Models and Life-Tables. *Journal of the Royal Statistical Society: Series B (Methodological)*. 1972;34(2):187-202.
38. Liberzon A, Birger C, Thorvaldsdóttir H, Ghandi M, Mesirov JP, Tamayo P. The Molecular Signatures Database (MSigDB) hallmark gene set collection. *Cell systems*. 2015;1(6):417-425.
39. Weber K, Thomaschewski M, Warlich M, et al. RGB marking facilitates multicolor clonal cell tracking. *Nat Med*. 2011;17(4):504-509.
40. Bolouri H, Farrar JE, Triche T, Jr., et al. The molecular landscape of pediatric acute myeloid leukemia reveals recurrent structural alterations and age-specific mutational interactions. *Nat Med*. 2018;24(1):103-112.
41. Ley TJ, Miller C, Ding L, et al. Genomic and epigenomic landscapes of adult de novo acute myeloid leukemia. *N Engl J Med*. 2013;368(22):2059-2074.